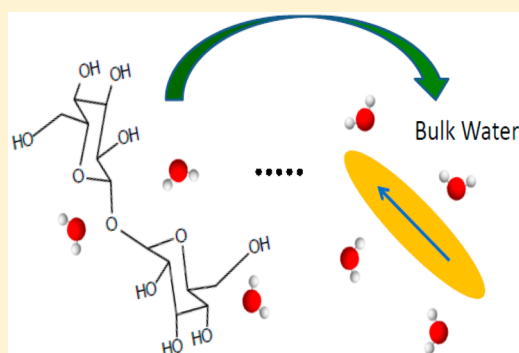


Retardation of Bulk Water Dynamics by Disaccharide Osmolytes

Nimesh Shukla,[†] Enrico Pomarico,[§] Lee Chen,[†] Majed Chergui,[§] and Christina M. Othon^{*,†,‡}[†]Department of Physics, Wesleyan University, Middletown, Connecticut 06457, United States[‡]Molecular Biophysics Program, Wesleyan University, Middletown, Connecticut 06457, United States[§]Laboratoire de Spectroscopie Ultrarapide (LSU) and Lausanne Centre for Ultrafast Science (LACUS), École Polytechnique Fédérale de Lausanne, ISIC, FSB, CH-1015 Lausanne, Switzerland

ABSTRACT: The bioprotective nature of disaccharides is hypothesized to derive from the modification of the hydrogen bonding network of water which protects biomolecules through lowered water activity at the protein interface. Using ultrafast fluorescence spectroscopy, we measured the relaxation of bulk water dynamics around the induced dipole moment of two fluorescent probes (Lucifer Yellow Ethylenediamine and Tryptophan). Our results indicate a reduction in bulk water reorganization rate of approximately 30%. We observe this retardation in the low concentration regime measured at 0.1 and 0.25 M, far below the onset of glassy dynamics. This reduction in water activity could be significant in crowded biological systems, contributing to global change in protein energy landscape, resulting in a significant enhancement of protein stability under environmental stress. We observed similar dynamic reduction for two disaccharide osmolytes, sucrose and trehalose, with trehalose being the more effective in reducing solvation dynamics.



■ INTRODUCTION

The importance of the physicochemical interactions of solvent molecules in regulating protein and biomolecular structural dynamics cannot be understated. Solvent molecules regulate protein folding and conformational stability by acting as a plasticizer, and it has been demonstrated that the dynamic behavior of a protein follows that of the hydration dynamics of the solvent.^{1,2} The maintenance of protein structure and activity in the cellular environment is carefully controlled by the relative concentration of small molecular osmolytes. These osmoprotectant molecules influence protein structure indirectly by regulating water activity and hydration dynamics. Small molecular solutes that influence water structure and dynamics can be roughly categorized into two groups labeled kosmotrope and chaotrope. Kosmotrope is a term used to describe molecules that stabilize protein structures through changes in water structure (“structure makers”), whereas chaotropes destabilize protein structures (“structure breakers”).³ A few examples of kosmotropic molecules are disaccharides, polyols, amino acids, and methylamines.

Disaccharide molecules, which are the focus of the current study, protect protein structures under a range of physical stresses including cryogenic temperature,^{4,5} elevated temperature,^{6–10} dehydration,^{11–15} and excessive salinity.^{15–17} Disaccharides are compatible osmolytes, meaning they do not perturb the native structure of proteins, nor are they limited to a particular structural folding motif or sequence; this makes them particularly useful for pharmaceutical and industrial purposes. Trehalose is the most effective disaccharide cryoprotectant and kosmotrope known. Trehalose is a nonreducing disaccharide of glucose linked through an α,α -(1

→ 1)-glycosidic bond, and is more effective at protecting biomolecular structure than other chemically similar disaccharides such as sucrose and maltose. A number of models have been proposed to explain the bioprotective properties of disaccharides. However, a complete picture of the physical mechanism of protection of protein structures remains elusive.

Several hypotheses have been formulated to explain the bioprotective effectiveness of disaccharides including the vitrification, preferential interaction, and water replacement models.¹⁸ The water replacement model applies only to systems under conditions of extreme dehydration. In this model, trehalose preferentially solvates biomolecules, thereby replacing water in the hydration layer.¹⁸ There is no evidence for a direct interaction between proteins and disaccharides in the hydrated state, and in fact, it has been demonstrated that disaccharides are preferentially excluded from the protein hydration layer.¹⁹ Therefore, we do not consider this model relevant to protein structural maintenance living systems under physiological conditions as presently studied. Both the vitrification and preferential solvation models imply that the disaccharides promote protein stability by slowing hydration dynamics and reducing water activity. There is ample experimental data to indicate retarded water dynamics within the hydration layer of disaccharides, including terahertz spectroscopy,²⁰ quasi-elastic neutron scattering (QENS) experiments,²¹ dynamic light scattering experiments,^{22,23} and NMR spectroscopy.²⁴ The vitrification model, however, cannot

Received: August 1, 2016

Revised: August 11, 2016

Published: August 15, 2016

explain the poor biopreservation properties of highly viscous (high glass transition temperatures) tetrasaccharides which share many of the physicochemical properties of the bioprotective disaccharides.^{25,26}

The preferential solvation model attributes the protective properties of disaccharides to strong cosolute–water interactions, which dramatically reduces water–water interaction in the bulk as well as water activity at the surface of the protein. Experimental evidence for preferential solvation exists in the Raman scattering signal for water–disaccharide mixtures.^{27,28} The results demonstrate an exceptional disruption of the hydrogen bonding network for trehalose concentrations above 30 wt %. Accordingly, it is hypothesized that trehalose reorders the bulk hydrogen bonding network more effectively than other solutes, resulting in dramatically slower dynamics and reduced water activity. This work also implies the existence of a critical disaccharide concentration beyond which the tetrahedral hydrogen bond network of water is significantly disrupted. We note, however, that the structural enhancement afforded by the trehalose for proteins under thermal stress appears to scale with sugar concentration (see Figure 1), and does not appear to exhibit a critical concentration dependence.

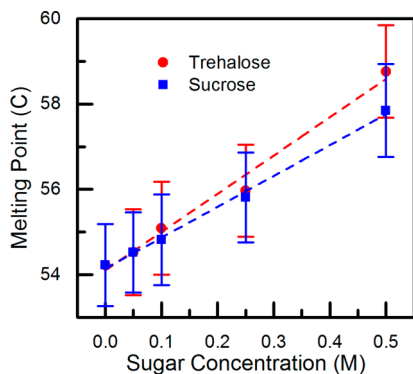


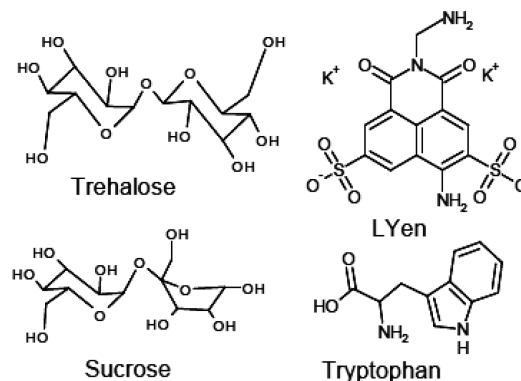
Figure 1. Melting temperatures for the enzyme Staph Nuclease as a function of increasing concentration of trehalose and sucrose.

The difference between the hydration of various disaccharides has also been probed by molecular dynamics simulation.^{27–32} Two studies in particular have compared disaccharides of glucose that differ only in their glycosidic bonds. Choi et al. compared 13 different disaccharides and found that trehalose was the most effective dynamic reducer of solvation layer dynamics.²⁹ They attributed this result to the rigidity of the molecule and the highly anisotropic distribution of water in the hydration layer. Vila Verde et al. also observed a superior reduction of water mobility in the solvation layer of trehalose, which they attribute to the topology of the molecule hindering water rotation in the solvation layer.³² Both groups, however, conclude that these effects should only impact dynamics in the first two hydration shells of the disaccharide and thus would not account for enhanced bioprotection by trehalose. Thus, there appears to be a disconnect between the biological enhancement of protein stability and the current measurements of water structure and bulk activity.

Importantly, most previous experiments have probed water dynamics near the disaccharide but do not attempt to measure hydration dynamics far from the disaccharide surface. The current study compares the hydration of small probe solutes in various low concentrations of trehalose and sucrose. We use

fluorescence frequency up-conversion to measure the relaxation of water around the excited state of two fluorophores: the dye molecule Lucifer yellow ethylenediamine (LYen) and the naturally fluorescent amino acid tryptophan.

Scheme 1. Chemical Structure of Molecules Used in This Work



EXPERIMENTAL METHODS

Sample Preparation and Characterization. The chemical structure of the molecules used in this study is given in Scheme 1. Tryptophan (99%), trehalose (99%), and sucrose (99%) were purchased from Acros Organic, Lucifer yellow ethylenediamine (94%) was purchased from Setarbiotech, and all were used without any further purification. All the solutions were prepared from ultrapure 18 MΩ water. The concentrations used for LYen and tryptophan experiments were 200 μM and 3 mM, respectively. All the measurements were taken at room temperature (~21 °C).

Steady State and Lifetime Measurements. Lifetime measurements were done on a time correlated single photon counting apparatus described in detail elsewhere.³³ In brief, a frequency doubled or tripled output of a high energy oscillator (Coherent Chameleon Ultra II) in conjunction with a pulse selector (Conoptics) was used to provide 425 or 295 nm pulses at 10.6 MHz repetition rate. The light was attenuated (to ~1.5 mw) and vertically polarized by passing it through a half wave plate and polarizer before exciting the sample in a quartz cuvette of 1 cm path length. The fluorescence collection was done at right angle geometry and passed through a precision linear polarizer placed at magic angle in order to isolate the effect of anisotropy from lifetime measurements. The collected light was focused onto the input slit of a Jerrell Ash (82-410) monochromator in order to filter the light at the fluorescence maximum of the probe. The output of the monochromator was then focused onto an avalanche photodiode (id100 ID Quantique). The residual infrared light was used to generate the synchronization signal which along with the output of the avalanche photodiode was fed to a single photon counting (TCSPC) module (Becker-Hickl SPC-130 TCSPC). The lifetime measurements were done at various concentrations of trehalose and sucrose for both LYen and Tryptophan. No difference in lifetimes was observed; data not shown.

Absorption spectra were recorded on a spectrophotometer (Beckman-650) by illuminating a 1 cm path length quartz cuvette. An inbuilt lamp as a stable light source (250–650 nm) and a photomultiplier tube were used for detection. The emission spectra were recorded on a spectrometer (Ocean

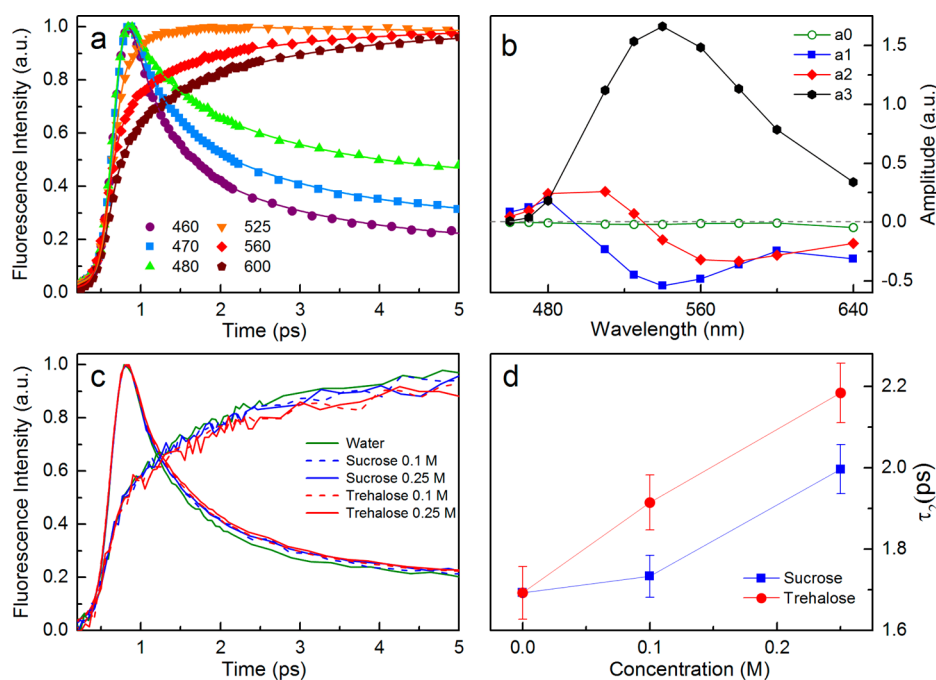


Figure 2. (a) LYen fluorescence up-conversion transients for wavelengths across the spectrum (points) and their global fit (solid line). (b) Amplitudes for global fit time constants (a0, a1, a2, and a3 are the amplitudes of Gaussian, fs, ps, and ns time constants, respectively). (c) Example up-conversion transients for various concentrations of disaccharides at 460 nm (fast decaying curves) and at 640 nm (slow rising curves). (d) Increase in the solvation time constant of LYen with respect to disaccharide concentration.

optics-QE65000) by exciting the sample in a quartz cuvette of path length 1 cm at its absorption maximum. The emitted fluorescence was collected at a right angle and fed onto the grating of the spectrometer using an optical fiber of length 2 m and diameter 0.6 mm (Ocean optics-QP600-2-SR). No measurable difference in absorption/emission spectra was found at various concentrations of disaccharides.

Fluorescence Frequency Up-Conversion. A high energy oscillator (Coherent Chameleon Ultra II) was used as the source of the fundamental beam. The laser output is tuned to 850 nm, with ~ 140 fs pulses at 80 MHz, giving 30 nJ/pulse. The output beam was split into equal parts to generate the pump and gate pulse trains. For the excitation beam, the fundamental beam was doubled using a 1.0 mm thick LBO crystal to provide 425 nm pump pulses of energy 1.2 nJ. The pump-beam polarization was set at the magic angle (54.7°) with respect to the up-conversion crystal axis to eliminate the influence of anisotropy on the signal. The pump pulses were focused onto a rotating circular cell (1 mm thickness) containing the sample. The forward-scattered fluorescence from excited samples was collected and focused by two 6 in. off-axis (90°) parabolic mirrors into a 0.5 mm thick BBO crystal (up-conversion crystal). A long-pass filter was placed between the mirrors to reject scattered laser light and pass the desired fluorescence signal. The gate pulses which were vertically polarized with an energy of ~ 10 nJ/pulse are passed through a computer-controlled optical delay line, and noncollinearly overlapped (at an angle of 10° for maximum efficiency) with the fluorescence signal in the up-conversion crystal. The efficiency was maximized by phase matching the angle of the up-conversion crystal. The up-converted signal, separated from the gate beam, was focused on the entrance slit of a 0.5 mm monochromator (oriel instrument-77250 series) equipped with a photomultiplier tube (Hamamatsu H9305-04) at the exit slit. The photomultiplier output was amplified using a lock-in

amplifier (SR530). An optical chopper running at 500 Hz was installed in the excitation beam as the reference signal for the lock-in. The up-converted transients were collected for 10 different wavelengths over the entire emission spectra. Sample fluorescence intensity and spectra were monitored using a fiber-coupled spectrometer (Ocean optics-QE65000) before and after the collection of up-conversion transients to check for sample degradation and photobleaching. No difference between spectra was observed. The instrumental response of the system was measured to be ~ 270 fs, from the Raman scattering of water.

An amplified laser system was required to generate the ultraviolet excitation for the measurement of tryptophan hydration dynamics. For this measurement, we used an up-conversion technique with broadband detection. A detailed description of the approach is given elsewhere.³⁴ Briefly, 290 nm pulses with a pulse width of 70 fs and a repetition rate of 130 kHz are generated from sum frequency mixing in a nonlinear optical parametric amplifier. The UV-excited emission signal is filtered with a 300 nm cutoff filter to remove the remaining excitation light, and then mixed in a BBO crystal with the 800 nm gate beam. The up-converted signal is detected with a monochromator equipped with a CCD camera. To achieve phase-matching, the sum frequency (SF) crystal is continuously turned to spectrally disperse the signal across the CCD array at each time delay. The broad-band measurements were carried out with a 250 μm BBO crystal, providing a time resolution of 180 fs as determined by a measurement of the Raman response from the solvent. In this system, the sample solution is pumped inside a 0.2 mm thick quartz flow cell. To avoid photodegradation, the sample flow and repetition rate were chosen to achieve one shot per spot. Moreover, the signal intensity and absorption spectrum were monitored for change after the measurement. The sample was at room temperature ($\sim 20^\circ\text{C}$). Before analyzing the time resolved fluorescence

spectrum, the Raman line of water was carefully removed from the data, using a Gaussian fit of the up-converted Raman band in pure water. Due to the small sample illumination area, the range of sugar concentration is limited. Significant caramelization and local heating can occur in dense sample fluids; given the limited window area of the flow cell, we restricted our study to 0.1 M.

Data Fitting Procedure. The transients shown in Figure 2c were globally fit using a sum of three exponential functions convoluted with the Gaussian instrument response function (IRF).³⁵ Time resolved emission spectra (TRES) for tryptophan shown in Figure 3 were obtained directly from

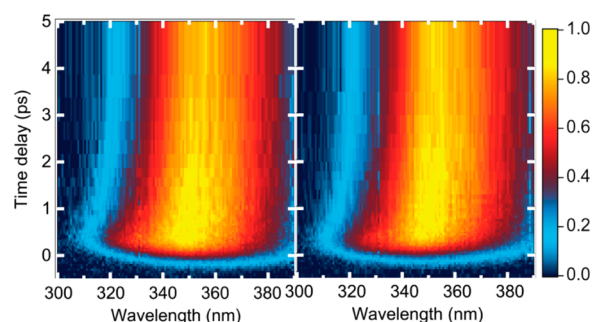


Figure 3. Spectral relaxation of tryptophan at 0.1 M concentration of disaccharides: (a) Trehalose; (b) Sucrose.

broadband frequency up-conversion and fit using a modified log-normal function.³⁶ The solvation time constants are directly correlated to the shift in the peak position of TRES with time. In order to extract the solvation relaxation time, the relaxation of the energy of the excited state (spectral first moment) is fit as a function of time. The time constants are reported in Table 1.

RESULTS AND DISCUSSION

Disaccharide Protection against Thermal Stress. The dependence of the melting temperature as a function of disaccharide concentration has been previously reported for multiple protein models.^{6–10,33,37} We verified this trend for both sucrose and trehalose using circular dichroism spectroscopy on a model protein system Staph Nuclease (SN). While both trehalose and sucrose stabilize the native structure of protein against thermal stress, trehalose appears to have a slightly larger slope as a function of increasing concentration; see Figure 1. Trehalose increases the melting temperature approximately 9 °C/M, while sucrose gives an increase of approximately 7 °C/M. If we take the onset of glassy dynamics to be the concentration at which bulk viscosity increases nonlinearly, then for both trehalose and sucrose, this onset is

found at concentrations close to 1.0 M. However, we can see from Figure 1 that even though error bars are large there is a significant enhancement in protein stability even at concentrations as low as 0.05 M, which is over an order of magnitude lower than that predicted by a vitrification model. We focused our experiments around the low concentration regime to see if there was a notable difference in water mobility, which would be indicative of dynamic inhibition of the hydrogen bonding network in the bulk caused by these disaccharides.

Measurement of Hydration Dynamics. Changes in the dynamic activity of water are probed using the dynamic Stokes shift of fluorescent probes. In order to accurately reflect the changes in solvation, the probe spectral properties cannot be impacted by the presence of the disaccharide cosolute. We measured the steady state emission spectra, the absorption spectra, and the lifetime of LYen and Tryptophan for disaccharide concentrations of 0, 0.1, and 0.25 M. No difference in emission/absorption spectrum or lifetime was found; this suggests that the disaccharide is not directly interacting with the probe, and any change in the probe dynamics is not due to an alteration of the excited state electronic configuration or solvent exposed area of the probe.

Fluorescence frequency up-conversion was used to measure dynamic changes due to bulk hydration dynamics. We measured the fluorescence transients of LYen at 10 wavelengths across the spectrum for 0, 0.1, and 0.25 M concentrations of trehalose and sucrose. We observe a fast decay on the blue side of the fluorescence maximum with a concomitant rise on the red side of the spectrum indicative of solvation of the excited state,³⁸ Figure 2a. In order to improve the signal quality, check for sample variation, and eliminate background noise, we measured multiple samples and used signal averaging to arrive at the reported hydration values. The use of a lock-in amplifier creates a time average of the signal level at each delay stage position. By collecting the signal intensity as a function of time, we collect a fluorescence transient at a particular signal frequency; 20–80 such transients were averaged to eliminate the influence of laser fluctuation and other systematic error. A minimum of two sets of data was taken independently and analyzed in order to ensure reproducibility among independent measurements. Finally, the obtained time constants from these data sets were averaged for each concentration. The values obtained for LYen were highly repeatable with fairly low uncertainty in the hydration time constants.

We analyzed our data using global fit (GF) of transients by one Gaussian and three exponentials (two solvation components and one lifetime component) convoluted with the instrument response function, Figure 2a. This form of spectral response has been widely investigated,^{39–42} and the attribution of these relaxation modes is discussed specifically for LYen by

Table 1. Time Constants Obtained for LYen and Tryptophan in the Presence of Trehalose and Sucrose at Various Concentrations

	conc.	Lucifer Yellow			Tryptophan	
		τ_0 (fs)	τ_1 (fs)	τ_2 (ps)	τ_1 (ps)	τ_2 (ps)
water	0	63.0 ± 0.8	390 ± 20	1.69 ± 0.05	0.16 ± 0.04 ^a	1.02 ± 0.12 ^a
sucrose	0.1	73.4 ± 0.8	340 ± 10	1.73 ± 0.04	0.2 ± 0.1	1.5 ± 0.4
sucrose	0.25	73.2 ± 0.7	390 ± 10	1.99 ± 0.04		
trehalose	0.1	73.1 ± 0.8	380 ± 10	1.91 ± 0.05	0.2 ± 0.2	1.4 ± 0.2
trehalose	0.25	69.8 ± 0.9	440 ± 20	2.18 ± 0.05		

^aBräm et al.⁴⁹

Vauthey et al. The results from the global fit for all LYen samples are given in Table 1. We are most interested in the solvent hydration which is described by the picosecond relaxation time scale. The lifetime component of 6.0 ± 0.1 ns was independently measured on a time correlated single photon counting (TCSPC) apparatus and was fixed during the global fitting for all samples of LYen.

The measured up-conversion transients and their global fits for LYen in pure water are shown in Figure 2a. For LYen in water, we observed two solvation components on a time scale of ~ 390 fs and ~ 1.69 ps. The shorter (\sim fs) component is due to vibration and libration energy loss.^{38,43,44} The few ps component is due to the solvation of the probe by water.^{38,43,44} From Figure 2b, we see the amplitude of the femtosecond and picosecond time constants changes sign from the blue to the red side of the spectrum, the signature of solvation.^{38,42} The amplitudes of the lifetime component remain positive across the spectrum, as expected. This approach to measuring solvation has been widely applied to analyze changes in water accessibility and hydrogen bond network dynamics.^{45–48}

Figure 2c displays representative transients for the probe molecule LYen in the presence of the two disaccharide cosolutes. In the presence of the sugars, the solvation of the excited state takes place at a slower rate on both the blue and red sides of the fluorescence spectrum. The difference is small but detectable across the fluorescence spectrum. We measured a solvation time constant of 1.99 ± 0.04 ps for trehalose and 1.73 ± 0.04 ps for sucrose at a concentration of 0.1 M and 2.18 ± 0.05 ps for trehalose and 1.91 ± 0.05 ps for sucrose at a concentration of 0.25 M. This is indicative of distinct retardation of dynamics in the bulk water by $\sim 30\%$ for trehalose and $\sim 15\%$ for sucrose at 0.25 M concentration. We observed an increase in solvation time constant with respect to disaccharide concentration, as shown in Figure 2d. Trehalose appears to have a larger slope than sucrose similar to the melting curve presented for Staph Nuclease, Figure 1, which is consistent with water mobility influencing the stability of protein structures as suggested by the preferential solvation model.

As a further exploration of the change in water activity around a solvated biomolecule, we chose to measure the Stokes shift around the naturally fluorescent amino acid tryptophan. This probe has excitation absorption maxima in the ultraviolet range, which is outside the doubled frequency range of the apparatus used for LYen. The full spectral response for both sucrose and trehalose at 0.1 M is shown in Figure 3. In order to extract solvation relaxation, the time resolved emission spectrum (TRES) at each delay time was fit with an asymmetric log-normal function. We extract the first moment of this fit and use it to monitor the spectral relaxation as a function of time, as shown in Figure 4.

The shift in the spectral maximum of TRES is directly correlated to solvation dynamics of tryptophan. We fit the relaxation curve with a three-exponential function convoluted with a Gaussian IRF of 250 fs in order to extract the solvation relaxation time constants. We use a fixed time constant of 3 ns representing lifetime of the probe. Using this method, we observed a solvation time constant of 1.4 ± 0.2 ps for trehalose and 1.5 ± 0.4 ps for sucrose. Previously, Bräm et al. reported a solvation time constant of 1.02 ± 0.12 ps for tryptophan in pure water.⁴⁹ We found the vibration component remains unchanged in the presence of sugars; however, the retardation in the hydration relaxation time constant around tryptophan

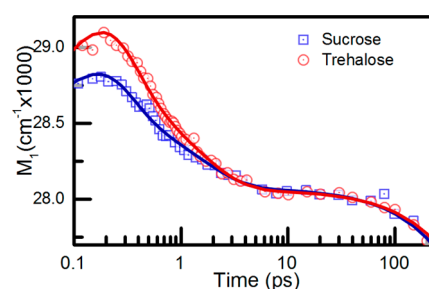


Figure 4. Spectral relaxation of tryptophan plotted as a function of time for 0.1 M trehalose and 0.1 M sucrose solutions; the error in the spectral fit is comparable to the size of the data point. A three-exponential fit convoluted with Gaussian IRF accurately represents the relaxation as shown (solid lines).

corresponds to a substantial decrease in dynamic activity of water in the bulk. This supports our observation in LYen that both disaccharides were successful in altering the dynamic activity of water in the bulk, far away from the disaccharide hydration layer.

Our results significantly extend the range at which retardation of hydration dynamics has to be detected. They complement with work done at much higher concentrations where the hydration layers of cosolutes are significantly overlapped. For example, Raman measurements of the water hydrogen bond angle are distorted for sugar concentrations above 1.0 M.^{27,28} More recently, the observations made by Sajadi et al.²⁰ suggest that for 0.4 M concentration of trehalose the solvation dynamics in the bulk are identical to those of a terahertz probe which is covalently bound to trehalose. From these results, they predict that the retardation of hydration dynamics should extend well beyond the solvation layer of the sugar. Our results support this prediction by showing retardation in bulk hydration dynamics in the low sugar concentration regime for solvated fluorescent probes. At this concentration (0.1 M), the average distance between molecules is approximately 21 Å which corresponds to ~ 7 layers of water.⁵⁰

CONCLUSIONS

This result is consistent with the categorization of these disaccharides as compatible cosolutes which are preferentially excluded from the protein surface.¹⁹ This study indicates that trehalose is effective in slowing hydration dynamics in the bulk. Although the large error in solvation time constant in the case of tryptophan restricts our ability to make a distinction between trehalose and sucrose, we observed a slightly stronger concentration dependent retardation of water activity for trehalose than sucrose in the case of LYen. Both disaccharides are effective in slowing dynamics of water and are effective bioprotective compatible osmolytes. This suggests that the alteration of water activity may be responsible for the linear enhancement in thermal stability for proteins observed for these disaccharides. Large differences in the thermal denaturation become apparent as the concentration is dramatically increased, and therefore, the role of viscoelastic and glassy dynamics may contribute significantly to the stabilization of large macromolecules in this concentration range. In conclusion, our results offer an indirect mechanism by which osmolyte molecules such as trehalose stabilize the protein structures by regulating the water activity at the protein surface while being preferentially excluded from this interface.

AUTHOR INFORMATION

Corresponding Author

*E-mail: cothon@wesleyan.edu. Phone: +18606852107.

Notes

The authors declare no competing financial interest.

ACKNOWLEDGMENTS

We thank Dr. Bertrand Garcia-Moreno E. (Johns Hopkins Department of Biophysics, Baltimore, MD) for generously providing the wild-type Staphylococcal Nuclease construct transformed into BL21(DE3) cells. We thank E. Taylor and her lab for their discussion and technical support. This work has been supported by the Connecticut Space Grant Consortium, and was partially funded by the NCCR:MUST of the Swiss NSF.

REFERENCES

- Reat, V.; Dunn, R.; Ferrand, M.; Finney, J. L.; Daniel, R. M.; Smith, J. C. Solvent Dependence of Dynamic Transitions in Protein Solutions. *Proc. Natl. Acad. Sci. U. S. A.* **2000**, *97*, 9961–9966.
- Halle, B. Protein Hydration Dynamics in Solution: A Critical Survey. *Philos. Trans. R. Soc., B* **2004**, *359*, 1207–1223 (discussion 1223–1204, 1323–1208).
- Yancey, P. H. Water Stress, Osmolytes and Proteins. *Am. Zool.* **2001**, *41*, 699–709.
- Somme, L. Anhydrobiosis and Cold Tolerance in Tardigrades. *Eur. J. Entomol.* **1996**, *93*, 349–357.
- Storey, K. B.; Storey, J. M. Frozen and Alive. *Sci. Am.* **1990**, *263*, 92–97.
- Lin, T. Y.; Timasheff, S. N. On the Role of Surface Tension in the Stabilization of Globular Proteins. *Protein Sci.* **1996**, *5*, 372–381.
- Xie, G.; Timasheff, S. N. The Thermodynamic Mechanism of Protein Stabilization by Trehalose. *Biophys. Chem.* **1997**, *64*, 25–43.
- Carninci, P.; Nishiyama, Y.; Westover, A.; Itoh, M.; Nagaoka, S.; Sasaki, N.; Okazaki, Y.; Muramatsu, M.; Hayashizaki, Y. Thermostabilization and Thermoactivation of Thermolabile Enzymes by Trehalose and Its Application for the Synthesis of Full Length Cdna. *Proc. Natl. Acad. Sci. U. S. A.* **1998**, *95*, 520–524.
- Sola-Penna, M.; Meyer-Fernandes, J. R. Stabilization against Thermal Inactivation Promoted by Sugars on Enzyme Structure and Function: Why Is Trehalose More Effective Than Other Sugars? *Arch. Biochem. Biophys.* **1998**, *360*, 10–14.
- Kaushik, J. K.; Bhat, R. Why Is Trehalose an Exceptional Protein Stabilizer? An Analysis of the Thermal Stability of Proteins in the Presence of the Compatible Osmolyte Trehalose. *J. Biol. Chem.* **2003**, *278*, 26458–26465.
- Wright Jonathan, J. C. Cryptobiosis 300 Years on from Van Leeuwenhoek: What Have We Learned About Tardigrades? *Zool. Anz.* **2001**, *240*, 563–582.
- Madin, K. A. C.; Crowe, J. H. Anhydrobiosis in Nematodes: Carbohydrate and Lipid Metabolism During Dehydration. *J. Exp. Zool.* **1975**, *193*, 335–342.
- Behm, C. A. The Role of Trehalose in the Physiology of Nematodes. *Int. J. Parasitol.* **1997**, *27*, 215–229.
- Crowe, J. H. The Physiology of Cryptobiosis in Tardigrades. *Mem. Ist. Ital. Idrobiol.* **1975**, *32*, 37–59.
- Newman, Y. M.; Ring, S. G.; Colaco, C. The Role of Trehalose and Other Carbohydrates in Biopreservation. *Biotechnol. Genet. Eng. Rev.* **1993**, *11*, 263–294.
- Purvis, J. E.; Yomano, L. P.; Ingram, L. O. Enhanced Trehalose Production Improves Growth of Escherichia Coli under Osmotic Stress. *Appl. Environ. Microbiol.* **2005**, *71*, 3761–3769.
- Hounsa, C. G.; Brandt, E. V.; Thevelein, J.; Hohmann, S.; Prior, B. A. Role of Trehalose in Survival of Saccharomyces Cerevisiae under Osmotic Stress. *Microbiology* **1998**, *144* (Pt 3), 671–680.
- Jain, N. K.; Roy, I. Effect of Trehalose on Protein Structure. *Protein Sci.* **2009**, *18*, 24–36.
- Lee, J. C.; Timasheff, S. N. The Stabilization of Proteins by Sucrose. *J. Biol. Chem.* **1981**, *256*, 7193–7201.
- Sajadi, M.; Berndt, F.; Richter, C.; Gerecke, M.; Mahrwald, R.; Ernsting, N. P. Observing the Hydration Layer of Trehalose with a Linked Molecular Terahertz Probe. *J. Phys. Chem. Lett.* **2014**, *5*, 1845–1849.
- Magazu, S.; Migliardo, F.; Telling, M. T. Alpha,Alpha-Trehalose-Water Solutions. VIII. Study of the Diffusive Dynamics of Water by High-Resolution Quasi Elastic Neutron Scattering. *J. Phys. Chem. B* **2006**, *110*, 1020–1025.
- Gallina, M. E.; Comez, L.; Morresi, A.; Paolantoni, M.; Perticaroli, S.; Sassi, P.; Fioretto, D. Rotational Dynamics of Trehalose in Aqueous Solutions Studied by Depolarized Light Scattering. *J. Chem. Phys.* **2010**, *132*, 214508.
- Uchida, T.; Nagayama, M.; Gohara, K. Trehalose Solution Viscosity at Low Temperatures Measured by Dynamic Light Scattering Method: Trehalose Depresses Molecular Transportation for Ice Crystal Growth. *J. Cryst. Growth* **2009**, *311*, 4747–4752.
- Hackel, C.; Zinkevich, T.; Belton, P.; Achilles, A.; Reichert, D.; Krushelnitsky, A. The Trehalose Coating Effect on the Internal Protein Dynamics. *Phys. Chem. Chem. Phys.* **2012**, *14*, 2727–2734.
- Crowe, J. H.; Carpenter, J. F.; Crowe, L. M. The Role of Vitrification in Anhydrobiosis. *Annu. Rev. Physiol.* **1998**, *60*, 73–103.
- Sussich, F.; Skopec, C.; Brady, J.; Cesàro, A. Reversible Dehydration of Trehalose and Anhydrobiosis: From Solution State to an Exotic Crystal? *Carbohydr. Res.* **2001**, *334*, 165–176.
- Lerbret, A.; Affouard, F.; Bordat, P.; Hedoux, A.; Guinet, Y.; Descamps, M. Low-Frequency Vibrational Properties of Lysozyme in Sugar Aqueous Solutions: A Raman Scattering and Molecular Dynamics Simulation Study. *J. Chem. Phys.* **2009**, *131*, 245103.
- Lerbret, A.; Bordat, P.; Affouard, F.; Guinet, Y.; Hedoux, A.; Paccou, L.; Prevost, D.; Descamps, M. Influence of Homologous Disaccharides on the Hydrogen-Bond Network of Water: Complementary Raman Scattering Experiments and Molecular Dynamics Simulations. *Carbohydr. Res.* **2005**, *340*, 881–887.
- Choi, Y.; Cho, K. W.; Jeong, K.; Jung, S. Molecular Dynamics Simulations of Trehalose as a 'Dynamic Reducer' for Solvent Water Molecules in the Hydration Shell. *Carbohydr. Res.* **2006**, *341*, 1020–1028.
- Corradini, D.; Strekalova, E. G.; Stanley, H. E.; Gallo, P. Microscopic Mechanism of Protein Cryopreservation in an Aqueous Solution with Trehalose. *Sci. Rep.* **2013**, *3*, 1218.
- Liu, Q.; Schmidt, R. K.; Teo, B.; Karplus, P. A.; Brady, J. W. Molecular Dynamics Studies of the Hydration of A,A-Trehalose. *J. Am. Chem. Soc.* **1997**, *119*, 7851–7862.
- Vila Verde, A.; Campen, R. K. Disaccharide Topology Induces Slowdown in Local Water Dynamics. *J. Phys. Chem. B* **2011**, *115*, 7069–7084.
- Chen, L.; Shukla, N.; Cho, I.; Cohn, E.; Taylor, E. A.; Othon, C. M. Sucralose Destabilization of Protein Structure. *J. Phys. Chem. Lett.* **2015**, *6*, 1441–1446.
- Cannizzo, A.; Bräm, O.; Zgrablic, G.; Tortschanoff, A.; Oskouei, A. A.; van Mourik, F.; Chergui, M. Femtosecond Fluorescence Upconversion Setup with Broadband Detection in the Ultraviolet. *Opt. Lett.* **2007**, *32*, 3555.
- Lang, B.; Angulo, G.; Vauthey, E. Ultrafast Solvation Dynamics of Coumarin 153 in Imidazolium-Based Ionic Liquids. *J. Phys. Chem. A* **2006**, *110*, 7028–7034.
- Maroncelli, M.; Fleming, G. R. Picosecond Solvation Dynamics of Coumarin 153: The Importance of Molecular Aspects of Solvation. *J. Chem. Phys.* **1987**, *86*, 6221.
- Kumar, A.; Attri, P.; Venkatesu, P. Trehalose Protects Urea-Induced Unfolding of Alpha-Chymotrypsin. *Int. J. Biol. Macromol.* **2010**, *47*, 540–545.
- Jimenez, R.; Fleming, G. R.; Kumar, P. V.; Maroncelli, M. Femtosecond Solvation Dynamics of Water. *Nature* **1994**, *369*, 471–473.

- (39) Furstenberg, A.; Vauthey, E. Ultrafast Excited-State Dynamics of Oxazole Yellow DNA Intercalators. *J. Phys. Chem. B* **2007**, *111*, 12610–12620.
- (40) Horng, M. L.; Gardecki, J. A.; Papazyan, A.; Maroncelli, M. Subpicosecond Measurements of Polar Solvation Dynamics - Coumarin-153 Revisited. *J. Phys. Chem.* **1995**, *99*, 17311–17337.
- (41) Furstenberg, A.; Kel, O.; Gradinaru, J.; Ward, T. R.; Emery, D.; Bollot, G.; Mareda, J.; Vauthey, E. Site-Dependent Excited-State Dynamics of a Fluorescent Probe Bound to Avidin and Streptavidin. *ChemPhysChem* **2009**, *10*, 1517–1532.
- (42) Furstenberg, A.; Vauthey, E. Excited-State Dynamics of the Fluorescent Probe Lucifer Yellow in Liquid Solutions and in Heterogeneous Media. *Photochem. Photobiol. Sci.* **2005**, *4*, 260–267.
- (43) Maroncelli, M.; Fleming, G. R. Computer Simulation of the Dynamics of Aqueous Solvation. *J. Chem. Phys.* **1988**, *89*, 5044.
- (44) Barnett, R. B.; Landman, U.; Nitzan, A. Relaxation Dynamics Following Transition of Solvated Electrons. *J. Chem. Phys.* **1989**, *90*, 4413.
- (45) Pal, S. K.; Zewail, A. H. Dynamics of Water in Biological Recognition. *Chem. Rev.* **2004**, *104*, 2099–2123.
- (46) Kwon, O. H.; Yoo, T. H.; Othon, C. M.; Van Deventer, J. A.; Tirrell, D. A.; Zewail, A. H. Hydration Dynamics at Fluorinated Protein Surfaces. *Proc. Natl. Acad. Sci. U. S. A.* **2010**, *107*, 17101–17106.
- (47) Othon, C. M.; Kwon, O. H.; Lin, M. M.; Zewail, A. H. Solvation in Protein (Un)Folding of Melittin Tetramer-Monomer Transition. *Proc. Natl. Acad. Sci. U. S. A.* **2009**, *106*, 12593–12598.
- (48) Xu, J.; Knutson, J. R. Ultrafast Fluorescence Spectroscopy Via Upconversion: Applications to Biophysics. *Methods Enzymol.* **2008**, *450*, 159–183.
- (49) Bram, O.; Oskouei, A. A.; Tortschanoff, A.; van Mourik, F.; Madrid, M.; Echave, J.; Cannizzo, A.; Chergui, M. Relaxation Dynamics of Tryptophan in Water: A UV Fluorescence up-Conversion and Molecular Dynamics Study. *J. Phys. Chem. A* **2010**, *114*, 9034–9042.
- (50) Winther, L. R.; Qvist, J.; Halle, B. Hydration and Mobility of Trehalose in Aqueous Solution. *J. Phys. Chem. B* **2012**, *116*, 9196–9207.